



Evaluation of the performance of corroded concrete with bottom ash and bacteria using resistivity and impact echo techniques

Ahmad Zaki^{1,2*}, Salma Azizah¹, Sri Atmaja P. Rosyidi¹, Khairil Mahbubi², Zainah Ibrahim³

¹Department of Civil Engineering, Faculty of Engineering, Universitas Muhammadiyah Yogyakarta, Indonesia

²Magister of Civil Engineering, Postgraduate Programme, Universitas Muhammadiyah Yogyakarta, Indonesia

³Department of Civil Engineering, Faculty of Engineering, University of Malaya, Malaysia

Abstract

Concrete is a significant contributor to global emissions, necessitating the development of environmentally friendly alternatives. This study explores the use of reinforced concrete (RC) incorporating industrial by-products, specifically bottom ash (BA), as a partial sand replacement to address this issue. Additionally, the study examines the potential of *Bacillus subtilis* bacteria to enhance the self-repair capabilities of corroded RC with BA. Concrete mixtures with 10%, 20%, and 30% BA were prepared and subjected to accelerated corrosion for 48, 96, and 168 hours. The corroded RC specimens were then tested for compressive strength, flexural strength, corrosion rate, non-destructive testing (NDT) methods, and SEM analysis. NDT methods included impact echo (IE) and resistivity techniques. Results showed that increasing BA content led to a decrease in corrosion resistance, with current measurements of 2.07, 1.64, and 1.47 amperes for 10%, 20%, and 30% BA, respectively. After 168 hours of corrosion, the IE frequency of the *Bacillus subtilis*-treated specimens was 2561.04 Hz, the lowest among all samples, while the 30% BA specimen exhibited the highest frequency at 7924.81 Hz. Resistivity measurements after 168 hours showed lower resistivity in *Bacillus subtilis*-treated specimens (18.25 k Ω -cm) compared to the 20% BA specimen (29.27 k Ω -cm). These findings suggest that the addition of BA and *Bacillus subtilis* bacteria can reduce the corrosion risk in concrete, making it a viable alternative to traditional RC.

This is an open access article under the [CC BY-SA](https://creativecommons.org/licenses/by-sa/4.0/) license



Keywords:

Bottom Ash;
Concrete;
Corrosion;
NDT Method;
Self-Healing;

Article History:

Received: May 19, 2024

Revised: August 18, 2024

Accepted: September 9, 2024

Published: May 1, 2025

Corresponding Author:

Ahmad Zaki

Magister of Civil Engineering,
Postgraduate Programme,
Universitas Muhammadiyah
Yogyakarta, Indonesia

Email: ahmad.zaki@umy.ac.id

INTRODUCTION

Concrete is a building material formed by hardening a mixture of fine aggregate, coarse aggregate (gravel or crushed stone), cement, water, air, and additives [1]. Concrete is a commonly used building material in civil engineering. Due to its widespread use, concrete contributes to greenhouse gas emissions and global warming [2][3]. A green revolution in the construction and industrial sectors is imperative to address the need for environmental conservation.

It is important to note that this is a potential solution; further research is necessary to determine its effectiveness. One possible solution is the use of eco-friendly concrete, which utilizes waste materials such as bottom ash (BA), fly ash (FA), silica fume (SF), and others to prevent global warming [4][5]. BA is rich in silica, calcium, aluminum, and iron [6]. BA also has high water retaining properties. The compressive strength of concrete with added BA is close to that of normal concrete with BA content below 10% [7]. Using BA

in the right amount can eliminate shrinkage cracks in concrete. FA, SF, and crystalline admixtures in different materials instead of cement were used to study the self-healing potential of mortar [8]. BA can eliminate shrinkage cracks and improve the self-healing capacity of concrete [9][10].

On the other hand, self-healing is one of the ingenious properties of hardened concrete, and all new and old structures remain strong even today with limited maintenance [11]. Repairing concrete with self-healing techniques with bacteria is becoming popular because it gives better results than other concrete methods [12][13]. This self-healing method can repair damage such as corrosion cracks and even prevent steel corrosion. Steel corrosion is a hazard that jeopardizes concrete function and life, especially in reinforced concrete (RC) [14]. Self-healing concrete materials can heal when cracked, but healing only occurs in small cracks. Cracks in concrete can cause corrosion due to the entry of harmful substances through these cracks, thus accelerating the corrosion of concrete reinforcement [15]. Repairing heavily corroded concrete reinforcement is costly and impacts the environment [16]. So, corrosion in RC needs to be inspected to prevent structural failure [17]. The non-destructive testing (NDT) method is one of the many inspection methods for corrosion monitoring of RC structures [18, 19, 20].

Research on corroded geopolymer concrete, especially BA with bacteria and evaluated using resistivity and impact echo, is rarely done. Much research has been done on the mechanical and other properties of concrete with BA as a replacement material [21, 22, 23, 24, 25]. There are limited studies about BA concrete with bacteria and only about fly ash and bacteria [26, 27, 28]. The research evaluated concrete with BA using NDT also limited to a few studies, i.e., ultrasonic pulse velocity (UPV) [29, 30, 31, 32], half-cell potential (HCP) [33], linear polarization resistance (LPR) [33], and rebound hammer [29]. This is related to research only by Morla et al. [33]. The study evaluated concrete with fly ash and BA using HCP and LPR techniques. The above NDT methods have their limitations regarding the results [20], so this study proposed using resistivity and impact echo. Resistivity can evaluate the ability of concrete to resist aggressive ions. For example, chloride ions and impact echo can detect defects in concrete due to the corrosion effect [19]. A combination of NDT resistivity and impact echo methods is potentially used for evaluating corroded concrete [17, 19, 34]. Therefore, the study assessed corroded concrete with BA and bacteria using resistivity and impact

echo, which is very important. In this study, the RC with *Bacillus subtilis* bacteria and BA with variations of 10%, 20%, and 30% are accelerated corrosion in 48, 96, and 168 hours. The corroded RC specimens are evaluated using resistivity and impact echo before and after corrosion.

METHOD

Material

The research was conducted at the Civil Engineering Laboratory of UMY. The fine aggregate material came from Kali Progo, the fine aggregate came from Clereng, the cement used was Portland type I with the Dynamix brand, and the water used in making the test specimens came from the UMY Civil Engineering Laboratory. The reinforcing bars used were plain reinforcing iron with a diameter of 12 mm and a length of 600 mm. The BA from the Central Java PLTU is shown in Figure 1a. The mixture of *Bacillus subtilis* bacteria developed in the UMY Agricultural Laboratory, as shown in Figure 1b.

This research uses formwork size 500 mm x 100 mm x 100 mm. In this study, 12 test specimens consisted of 3 normal concrete and 9 concrete mixes of BA and self-healing along with corrosion levels on the test specimens.

Raw Materials

The purpose of raw material testing using SEM-EDX is to examine the surface morphology and sample composition at the micro-scale or nanoscale level. By combining Scanning Electron Microscopy (SEM) and Energy Dispersive X-ray Spectroscopy (EDX), the technique can provide valuable information about the morphology, structure, and composition of materials, as well as enable failure analysis, mineralogy, and biological research. These tests help determine the quality of the material, identify the chemical elements contained, and understand the process of material formation. In this test, samples weighing at least 0.5 grams were used as a powder from raw material BA. The test results can be seen in Figure 2 and Figure 3.

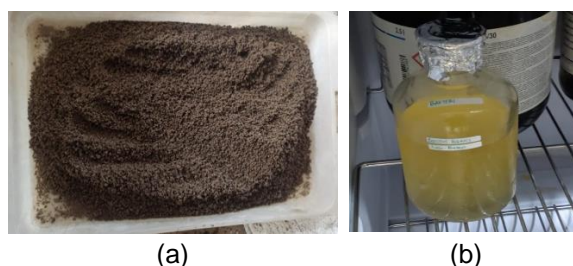


Figure 1. (a) Bottom ash and (b) Bacteria *Bacillus subtilis*

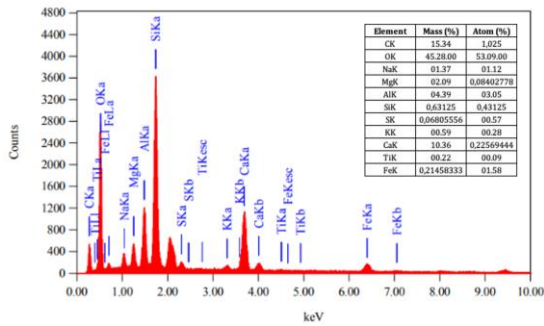
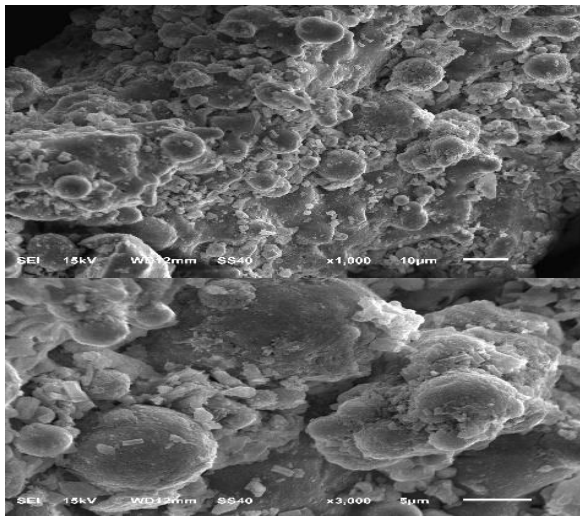


Figure 2. SEM-EDX of Bottom Ash

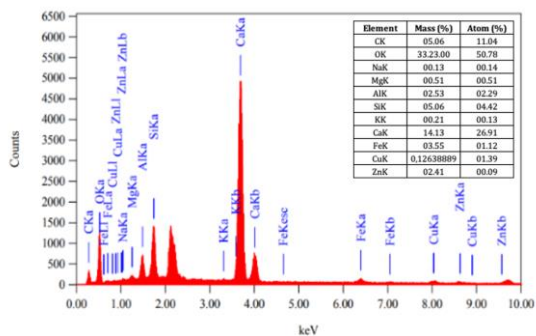
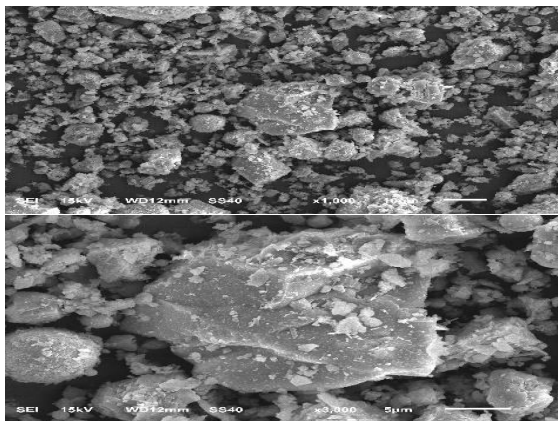


Figure 3. SEM-EDX of Cement

The SEM-EDX test reveals morphological patterns in the form of small, spherical particles on Coal Bottom Ash (CBA) under 1000x magnification, whereas the BN test objects exhibit irregular shapes. The goal of EDX (Energy Dispersive X-ray Spectroscopy) testing is to determine the sample's elemental composition. The elements in the BA material are C (carbon), O (oxygen), and Si (silicon), containing Mg, K, Ca, S, Na, and Al. In cement material, the elements produced are C (carbon), O (oxygen), and Ca (calcium), containing Na, Mg, Al, Si, K, Fe, Cu, and Zn. The percentage of silica in cement material is 5.08%, a lower percentage than in BA material, with the highest percentage of 14.69%. This indicates that the grains in BA are finer than cement and have a different arrangement of elements. Calcium in cement, the most abundant element, is found in BA at 44.13%, up to 10.36%.

Material Testing

Material tests were conducted on coarse and fine aggregates. For fine aggregates, the specific gravity and water absorption of fine aggregates were tested based on the Indonesian National Standard (SNI) 1970:2008 and SNI 1969:2008, and the mud content of fine aggregates was tested based on SNI ASTM C117:2012. For coarse aggregates, the material tests carried out are testing the specific gravity and water absorption of coarse aggregates based on SNI 1969:2016, testing the mud content of coarse aggregates based on SNI 03-4142-1996, and testing the wear of coarse aggregates based on SNI 03-4142-1996. The test results can be seen in Table 1, where the results have met the requirements of the concrete constituent materials.

Table 1. Aggregate test result data

Test Type	Fine Aggregate	Coarse Aggregate	Unit
Fine Modulus	2.435		-
Bulk specific gravity	1.837	2.642	-
Saturated surface dry specific gravity	2.242	2.707	-
Apparent specific gravity	3.094	2.826	-
Water absorption	22.165	2.456	%
Mud content	1	1	%
Abrasion		15.75	%

Mix Design Concrete

The mix design calculation is guided by ACI 211.1-91, with a planned compressive strength of 30 MPa and a safety factor of 40%. The data was obtained from testing materials such as sand and gravel and used to prepare the concrete-making

mixture. The proportion of Bacillus subtilis bacteria added was 10^5 cfu/ml of water per specimen. The mix design of the specimen can be seen in Table 2 and Table 3.

Specimen Fabrication

The specimen was a reinforced concrete (RC) beam measuring 500 mm x 100 mm x 100 mm with a reinforcement diameter of 12 mm and a length of 600 mm, as shown in Figure 4. The reinforcement was extended more than the beam size to facilitate the accelerated corrosion method. A cylindrical specimen measuring 300 mm x 150 mm was made for the compressive strength test. Bacteria were mixed directly at the time of making the specimens.

Compressive Strength and Flexural Strength Test

Tests are carried out using a Universal Testing Machine (UTM) tool to determine the compressive strength of concrete specimens. This test is carried out on concrete cylinders that have passed the curing process for 28 days. Testing the flexural strength of concrete using a Universal Testing Machine (UTM) after the corrosion process is complete. The tests were conducted at the Structures and Construction Materials Laboratory, Civil Engineering, UMY. The test was carried out with two loading points in the middle of the beam span and 5 cm between the support and the edge of the beam.

Corrosion Acceleration Testing

This test was conducted on RC cured for 28 days. The corrosion process was accelerated using a DC Power Supply to distribute the electric current. The rebar was connected to the positive pole, while the sacrificial rebar was connected to the negative pole and immersed in a 5% NaCl solution. The percentage of corrosion was determined by calculating the percentage of mass loss in the rebar using Faraday's Law [35]. This

process was carried out for 48 hours, 96 hours, and 168 hours on beam specimens.

Resistivity and Impact Echo Testing

Resistivity testing was conducted to obtain the quality of the concrete before the accelerated corrosion process. This process was carried out on 28-day-old specimens. This process is carried out on the specimen, which can be known compared to the results before corrosion. Resistivity testing at each point is done three times so that the data obtained is complete and more accurate. Impact echo tests are helpful for measuring the thickness of a structural layer and detecting gaps in the structure. Tests are conducted on concrete specimens to detect defects in concrete.

RESULTS AND DISCUSSION

Slump Test Results

The slump test results, based on SNI 2493:2011, show that as the percentage of bottom ash (BA) in the concrete mixture increases, the slump value decreases. This can be attributed to BA's higher water absorption compared to natural coarse aggregates, increasing the water demand and lowering the workability of the mixture [36]. Figure 5 illustrates the slump values at varying BA percentages.

Table 2. Mix design concrete per 1 m³

Material	Total	Units
Sand	641.398	kg
Gravel	984.75	kg
Cement	484.213	kg
Water	205	liter

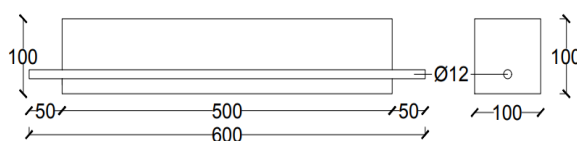


Figure 4. Beam test specimen (in mm)

Table 3. Mix design concrete per specimen

Specimen	Bottom Ash (%)	Bottom Ash (Kg)	Sand (Kg)	Gravel (Kg)	Cement (Kg)	Water (Kg/L)	Basillus Subtilis (cfu/ml)
BN1	0	0.00	4.49	6.89	3.39	1.43	10 ⁵
BN2	0	0.00	4.49	6.89	3.39	1.43	
BN3	0	0.00	4.49	6.89	3.39	1.43	
BS1	10	0.43	3.90	6.89	3.39	1.43	
BS2	10	0.43	3.90	6.89	3.39	1.43	
BS3	10	0.43	3.90	6.89	3.39	1.43	
BS4	20	0.86	3.47	6.89	3.39	1.43	
BS5	20	0.86	3.47	6.89	3.39	1.43	
BS6	20	0.86	3.47	6.89	3.39	1.43	
BS7	30	1.30	3.03	6.89	3.39	1.43	
BS8	30	1.30	3.03	6.89	3.39	1.43	
BS9	30	1.30	3.03	6.89	3.39	1.43	

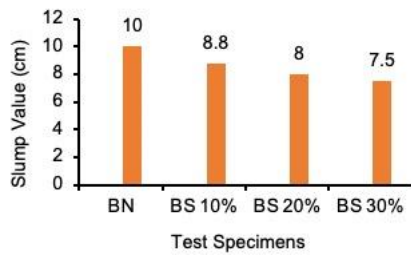


Figure 5. Slump test results

The results align with previous studies by Chindasiriphan, et al. [22], which also noted a similar decrease in workability with the inclusion of BA in concrete mixtures due to its pozzolanic nature. This observation indicates that optimizing the BA content is crucial for balancing workability and strength.

Compressive Strength Test

Data on the compressive strength test results on cylindrical specimens can be seen in Table 4. Table 4 and Figure 6 show that compressive strength results in normal concrete producing the highest compressive strength values compared to concrete using BA mixtures. Meanwhile, the 20% variation of the BA mixture and 10 ml bacteria increased the compressive strength by 1.47 MPa. Meanwhile, the 30% BA variation test specimen decreased by 3.06 MPa. This may occur because the optimum BA mixture in the manufacture of concrete has a 20% BA variation, so the 30% variation of concrete decreases the compressive strength value.

The compressive strength of normal concrete is higher than that of concrete, which several factors can cause. Some studies have shown that the reaction of pozzolan after cement hydration takes a long time, thus increasing the strength of concrete.

Table 4. Data of compressive strength test results of cylindrical specimens

Specimens	Bottom Ash (%)	Compressive strength (MPa)	Average Compressive Strength (MPa)
BN1	0	39.59	37.59
BN2		37.22	
BN3		35.97	
BS1	10	35.13	33.44
BS2		32.97	
BS3		32.23	
BS4	20	34.32	34.91
BS5		34.72	
BS6		35.69	
BS7	30	29.91	31.85
BS8		30.26	
BS9		35.38	

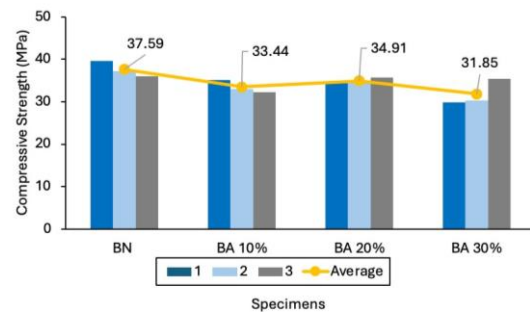


Figure 6. Concrete compressive strength results

However, at low replacement percentages, the amount of silica in the pozzolan is low, which can cause a decrease in strength. In addition, the workability of concrete decreases as the pozzolan content increases, which can affect the concrete's overall strength. According to Abdullah et al. [37] Compressive strength may decrease as the percentage of BA increases, but this decrease is generally gradual and insignificant. It should also be noted that the large amount of pozzolan content in concrete causes slow separation of granular particles, decreasing the density and strength of the concrete material.

Corrosion Acceleration Testing

The acceleration process is carried out for 48, 96, and 168 hours on the beam specimen. The acceleration graph can be seen in Figure 7. The 48-hour acceleration duration graph results in Figure 7a show that the BN specimen increased at 16 hours, and after 17 hours, the current increased significantly. This is possible due to current leakage from the DC power supply or the current flow not effectively channeled to the reinforcement. The average current in the 20% optimum BA variation specimens is lower than in the BN specimens.

Meanwhile, in the 10% and 30% BA variation specimens, the average current is higher than that of the BN specimens. This is influenced by the optimum level of BA mixture in the specimens. Concrete with non-optimum pozzolanic admixtures can experience high corrosion rates [38]. After the acceleration process, the concrete was demolished to take the reinforcement inside the concrete to be weighed and determine the actual weight. After crushing, the reinforcement is cleaned from the remnants of the destroyed concrete from the rust attached to the reinforcement. The calculation of the estimated weight loss of the reinforcement can be seen in Table 5. The reinforcement weight before corrosion is 500 grams.

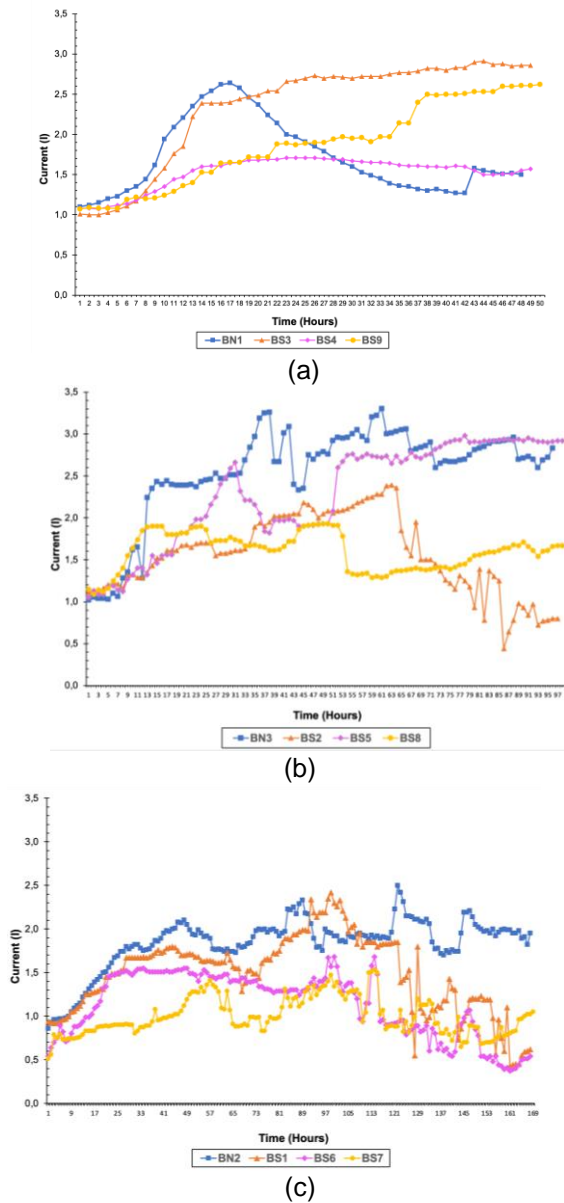


Figure 7. Acceleration graphs of (a) 48 hours, (b) 96 hours, and (c) 168 hours

Table 5. Mass loss results and actual corrosion rate

Specimens	Current (I)	Acceleration duration (hour)	Mass Loss Estimation (gr)	Corrosion Level Estimation (%)
BN1	1.70	48	85.03	17.01
BN2	1.84	168	322.02	64.40
BN3	3.25	96	326.13	65.23
BS1	2.36	168	260.70	52.14
BS2	1.55	96	156.11	31.22
BS3	2.31	48	115.95	23.19
BS4	1.51	48	75.95	15.19
BS5	2.29	96	229.51	45.90
BS6	1.13	168	197.97	39.59
BS7	1.00	168	175.49	35.10
BS8	1.56	96	160.10	32.02
BS9	1.85	48	93.74	18.75

In reinforcement that has passed the corrosion process, the cross-sectional area of the reinforcement will decrease. This occurs due to local corrosion (pitting), which causes the diameter of the reinforcement to decrease [39]. In this study, the reduced diameter of the reinforcement was measured every 5 cm along the length of the reinforcement. Figure 8 is a graph of the measurement of diameter reduction in the reinforcement.

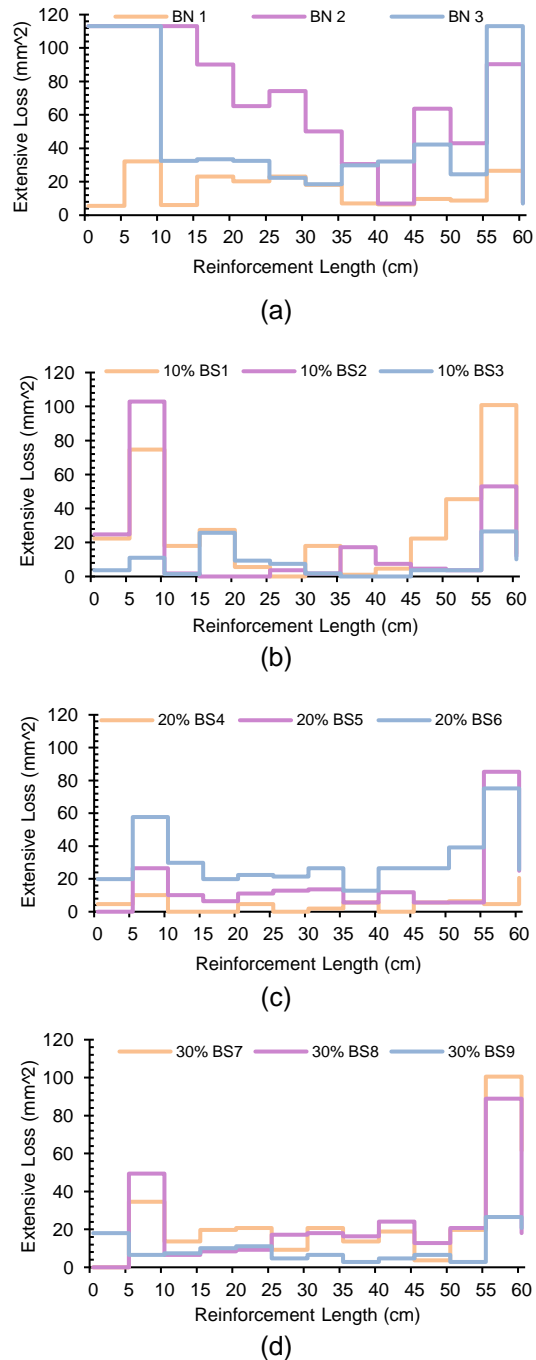


Figure 8. Diameter reduction in reinforcement (a) BN, (b) BA 10%, (c) BA 20%, and (d) BA 30%

In this study, the measurement results of reinforcement diameter reduction of test specimens (a) BN, (b) BA 10%, (c) BA 20%, and (d) BA 30% were obtained. The graph in Figure 8 (a) BN shows that the reduction in diameter or cross-sectional area of the reinforcement is more significant when compared to the BA specimen. This can be interpreted as concrete with BA admixture protecting it from the corrosion process, which will cause the diameter or cross-sectional area of the reinforcement to decrease.

Table 6 shows the results of mass loss and actual corrosion rate. In this test, the best corrosion resistance was observed in the 20% variation specimens with corrosion rates of 9.8%, 5.2%, and 7.4% at each acceleration duration.

**Non-Destructive Testing (NDT)
Impact Echo Testing**

Impact-echo (IE) testing aims to indicate the durability of the specimen and the thickness of the specimen layer, as well as detect any gaps or voids in the test piece. From the results of IE testing, amplitude, and frequency data are obtained in this test using 4 spacing sensors with 5 cm, 10 cm, 15 cm, and 20 cm on each specimen. The results of the frequency and amplitude graph can be seen in Figure 9. Based on the IE tests that have been carried out, the frequency and amplitude values of the BN specimens have lower frequency values. Pozzolanic concrete has a higher maximum frequency than normal concrete, which affects the ability of the IE waves produced [17]. Figure 10 generally shows that the higher the frequency value, the lower the corrosion rate, as indicated by the frequency value at 48 hours. The corrosion time has a frequency greater than 96 hours and 168 hours. This frequency value is very influential on the corrosion rate of the specimen. However, the frequency value fluctuates, or the development is not fixed.

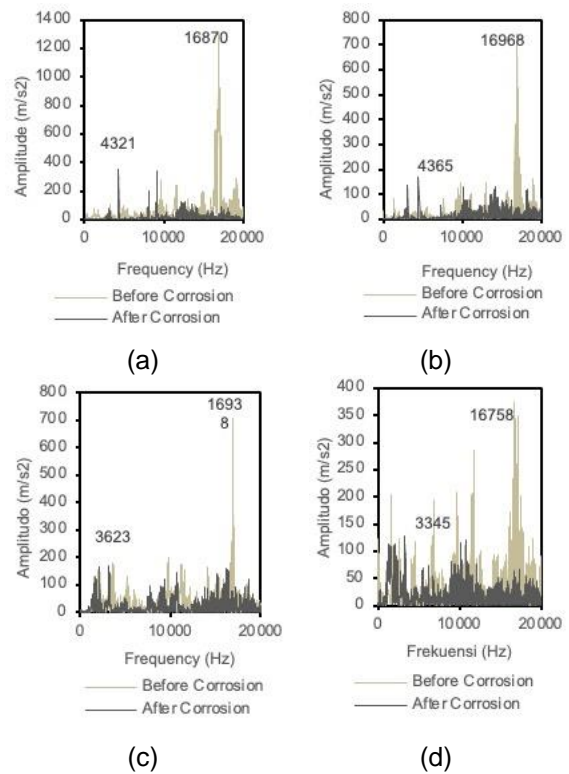


Figure 9. IE graph of BS1 at sensor distance (a) 5 cm, (b) 10 cm, (c) 15 cm, and (d) 20 cm

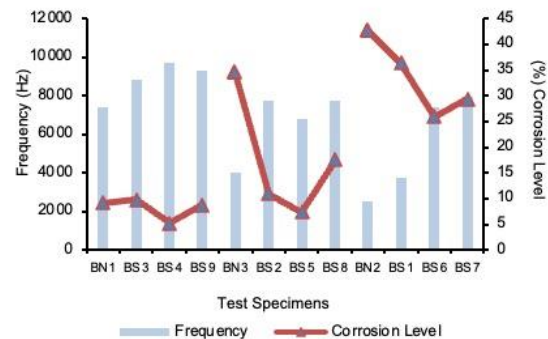


Figure 10. Relationship between IE frequency value and corrosion rate

Table 6. The results of the corrosion test

Specs	Final Weight (gr)	Actual corrosion rate (%)	Mass Loss Estimation (gr)	Actual Mass Loss (gr)	Deviation (%)
BN1	454	9.2	85.03	46	7.81
BN2	287	42.6	322.02	213	21.80
BN3	327	34.6	326.13	173	30.63
BS1	318	36.4	260.70	182	15.74
BS2	445	11	156.11	55	20.22
BS3	451	9.8	115.95	49	13.39
BS4	474	5.2	75.95	26	9.99
BS5	463	7.4	229.51	37	38.50
BS6	370	26	197.97	130	13.59
BS7	353	29.4	175.49	147	5.70
BS8	412	17.6	160.10	88	14.42
BS9	456	8.8	93.74	44	9.95

Table 7 shows that at a corrosion time of 48 hours, the normal specimen has the lowest frequency of 7381.59 Hz, and the highest is 9692.38 Hz in 20% BA concrete. At a corrosion time of 96 hours, normal concrete has the lowest frequency of 4033.2 Hz, and in this BA, concrete gets a frequency that is not much different around 7000s, with the highest 10% BA concrete of 7769.78 Hz. At a corrosion time of 168 hours, normal concrete with the lowest frequency of 2561.04 Hz also has the highest actual corrosion.

Table 7. Impact echo test results

Specs	Corrosion time (hour)	Actual Corrosion (%)	Freq. before corrosion (Hz)	Freq. after corrosion (Hz)
BN1	48	9.2	10626.22	7381.59
BN2	168	42.6	10084.23	2561.04
BN3	96	34.6	9825.44	4033.2
BS1	168	36.4	16970.22	3787.84
BS2	96	11	16459.96	7769.78
BS3	48	9.8	18508.30	8836.67
BS4	48	5.2	18792.73	9692.38
BS5	96	7.4	17824.71	6807.89
BS6	168	26	17331.54	7440.19
BS7	168	29.4	17617.19	7924.81
BS8	96	17.6	17037.35	7751.47
BS9	48	8.8	17619.63	9337.16

In BA concrete, as the percentage of BA 10%, 20%, and 30% is added, the higher the frequency value is successively 3787.84, 7440.19, and 7924.81 Hz. From these data, it is concluded that the addition of BA can increase the frequency and then withstand the corrosion rate better than normal concrete.

The relationship between corrosion rate and IE value in concrete is an indirect influence, but it can indicate the deeper condition of the concrete. This shows that the corrosion rate can affect the remaining thickness of the steel profile, which can be detected through IE testing. Figure 11 shows the relationship between frequency and corrosion rate.

The correlation coefficient is 0.7118, which is close to 1, meaning that there is a relationship between frequency and corrosion rate. The frequency value has a positive correlation with the corrosion rate. When the frequency value decreases, the corrosion rate of the specimen will be higher. This is because the IE method is very sensitive to damage due to carbonation and corrosion [40].

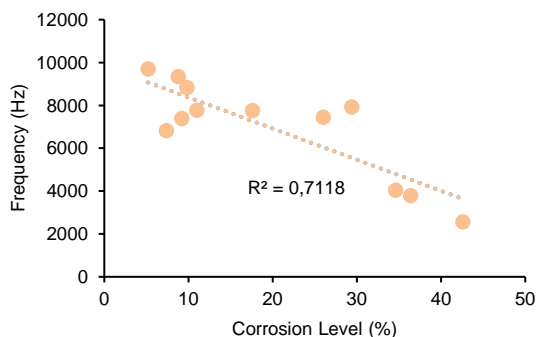


Figure 11. Relationship between frequency and corrosion rate

Resistivity Testing

The purpose of resistivity testing is to determine the electrical resistance value of concrete test specimens. The test is carried out in two stages, before and after corrosion, so that the data can be analyzed and compared with the results of the corrosion process [34]. Specimens have passed the curing process with a quality plan of 30 MPa. Based on Table 8, the resistivity results obtained before corrosion on BN and BS1-BS9 test specimens, the resistivity value is in the very low category or not smaller than 37 kΩ-cm. After being corroded for 48 hours, a decrease in resistivity also occurred. The resistivity of normal concrete and 10% BA was not much different, namely 29.02 and 30.14, then increased to 40.89 and 37.07 at 20% and 30% BA. At a corrosion time of 96 hours, normal concrete gets the lowest resistivity of 20.56, and the highest is still at 20% BA of 37.35. Then, in the case of 168 hours of corrosion time, normal concrete also remained the lowest at 18.25, and the highest remained in concrete with the addition of 20% BA at 29.27. The resistivity results show that the addition of BA to concrete can increase resistivity or show a smaller level of corrosion risk than normal concrete. The results of the resistivity calculation and the actual corrosion rate are plotted on a graph in Figure 12.

The resistivity value of the BA and bacteria mixture specimens and the resistivity value of the BS specimens in all variations are higher than normal concrete. The resistivity value of pozzolan concrete is higher than normal concrete because pozzolan can reduce the porosity of concrete and form more stable silicate compounds. Pozzolan concrete will increase concrete compressive strength and durability and reduce corrosion rates [41]. The results show that the specimens with a BA mixture can improve the resistivity value and prevent the specimens from corrosion.

Table 8. Resistivity test results

Specs	Corrosion time (hour)	Actual corrosion (%)	Resistivity before corrosion	Resistivity after corrosion
BN1	48	9.20	38.59	30.14
BN2	168	42.60	37.31	18.25
BN3	96	34.60	38.09	20.56
BS1	168	36.40	67.82	22.84
BS2	96	11.00	65.87	26.41
BS3	48	9.80	71.86	29.02
BS4	48	5.20	68.51	40.89
BS5	96	7.40	73.10	37.35
BS6	168	26.00	69.67	29.27
BS7	168	29.40	60.14	25.58
BS8	96	17.60	73.00	27.54
BS9	48	8.80	71.66	37.07

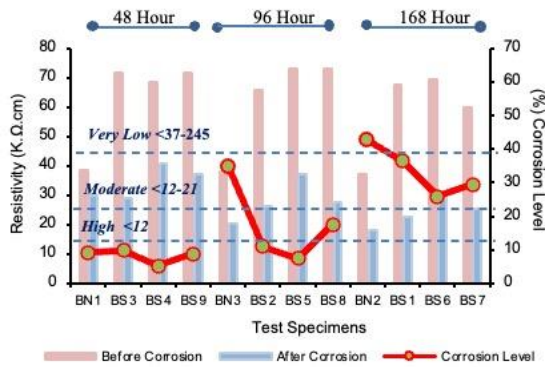


Figure 12. Resistivity and corrosion rate relationship graph

Figure 13 shows the relationship between the corrosion rate and resistivity value, where if the resistivity value is lower, the corrosion rate will be higher, and vice versa. If the resistivity value is high, the corrosion rate will be low. The effect occurs due to the ability of concrete to conduct electric current through the material. If the resistivity value of the concrete is high, the electric current entering the concrete material will be lower, which will affect the corrosion rate of the concrete. From Figure 13, a correlation value of >70% is obtained, indicating that there is a high relationship between the resistivity value and the corrosion rate.

Flexural Strength Testing

This test was conducted on a corroded beam specimen that had undergone an accelerated corrosion process. In SNI 4154: 2014, the test was carried out using the centered loading method in the middle of the rod to determine the acceptable free capacity. Data on the results of the flexural strength test on beam specimens after the acceleration process can be seen in Table 9.

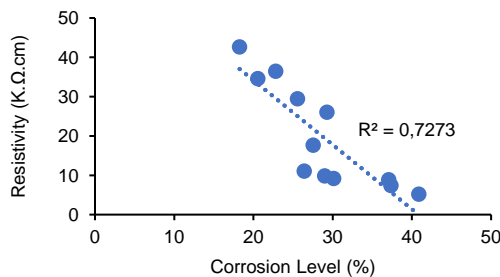


Figure 13. Graph of the relationship between corrosion rate and resistivity value

Table 9. Flexural strength results after corrosion

Spec.	Stress (kgf)	Corrosion Duration (hours)	Actual corrosion level (%)	Flexural strength (MPa)
BN1	1867.4	48	9.2	12.53
BN2	934.58	168	42.6	6.46
BN3	1163.4	96	34.6	7.96
BS1	829.83	168	36.4	5.64
BS2	1575.3	96	11	10.73
BS3	1769	48	9.8	11.61
BS4	2014.1	48	5.2	13.43
BS5	1138	96	7.4	7.66
BS6	595.93	168	26	3.85
BS7	551.19	168	29.4	3.49
BS8	661.02	96	17.6	4.41
BS9	1753.5	48	8.8	12.16

The highest flexural strength value at 48 hours duration is in the BS4 specimen with 20% BA variation. At a duration of 96 hours, the flexural strength value was at 10% variation of the BS2 specimen. Meanwhile, at a duration of 168 hours, the highest flexural strength value is in the normal concrete specimen BN2. In the 30% variation of BA test specimens, the flexural strength value is lower when compared to normal concrete. The flexural strength of concrete decreases as the corrosion process increases. This occurs because the flexural strength is strongly influenced by the acceleration process, as can be seen in Figure 14.

Self-Healing Process

The self-healing concrete process was carried out for 28 days after the accelerated corrosion and flexural strength tests on the beam specimens. The method used is by mixing bacteria into a fresh concrete mixture of 10 ml. The self-healing process was observed in 7 days, 14 days, and 28 days. The self-healing process can be seen in Figure 15.

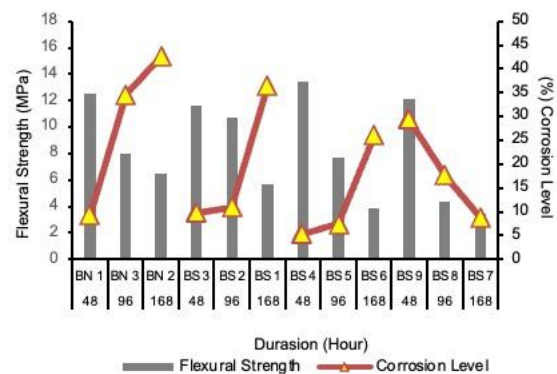


Figure 14. Diagram of flexural strength test results of corroded specimens

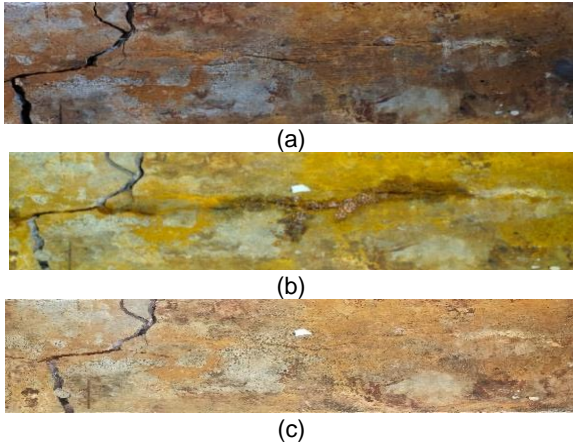


Figure 15. Self-healing process of BA 10% BS1 (a) 7 days observation, (b) 14 days, and (c) 28 days

From the observations that have been made on BA concrete specimens for 28 days on beam specimens that have cracked. The results show that self-healing in all variations of concrete with BA admixture does not work optimally. When concrete cracks, bacteria present in concrete, such as *Bacillus subtilis*, will become dormant spores in extreme environments, too acidic concrete, bacteria may not be able to survive and heal cracks effectively. The spores produced by *Bacillus subtilis* bacteria can survive in concrete for 200 years, and they will be active when exposed to water and oxygen [42, 43, 44].

Therefore, it is important to ensure that the pH level of the concrete is within a range that supports bacterial growth and survival. In addition, the study by Wong et al. [45] highlighted the importance of protecting bacteria in concrete to maintain their self-healing ability over the life of the concrete. If bacteria are not encapsulated, it is possible they may not be able to survive in the harsh environment of concrete, which could lead to ineffective self-healing. According to the results of Nindhita et al. [46], adding bacterial encapsulation to reinforced concrete can reduce corrosion. Encapsulating bacteria in materials such as expanded clay can help protect bacteria and ensure their long-term survival.

Micro-structure

In SEM microstructure testing, concrete specimens with a corrosion acceleration duration of 168 hours are used. The specimen used in this test is BA mixed concrete using self-healing and normal concrete. The SEM test results can be seen in Figure 16 and Figure 17.

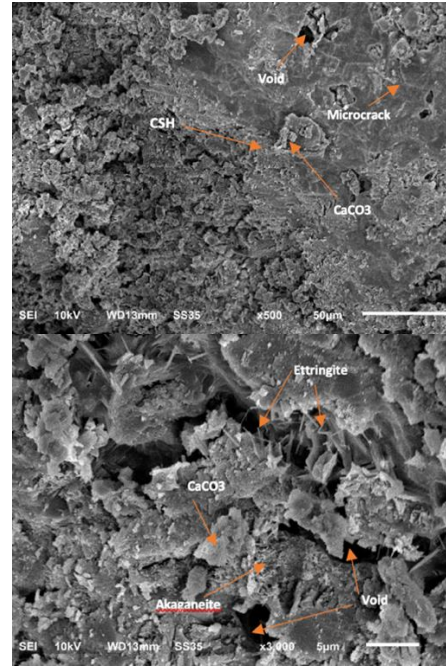


Figure 16. SEM of BN Specimen

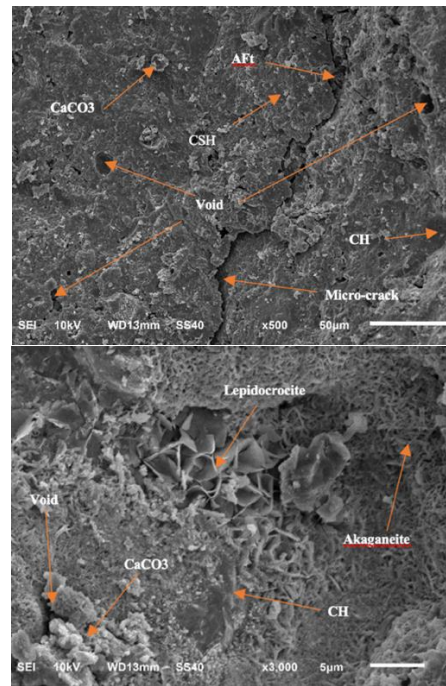


Figure 17. SEM of BS Specimen

Ettringite in SEM can be complex and shaped like fibers or small needles; ettringite can also be called the AFt phase [47]. The CH (Calcium Hydroxide) form can be seen as a dark hexagonal-shaped structure, occupying about 20-25% of the volume of cement paste, and does not contribute strength to the cement [47]. Pores are empty spaces contained in concrete structures. Pores can be dark hollows, while hair cracks are fractures in the dark phase. The comparison of

calcium silicate hydrate (C-S-H) produced by normal concrete and BA shows that the addition of BA can reduce the quality of C-S-H. In several studies and literature reviews conducted, the results show that the addition of BA can reduce the compressive strength of concrete, which is caused by the presence of contaminants in BA that interfere with the cement hydration process and produce less effective C-S-H. The addition of BA can reduce the compressive strength of concrete because the properties of pozzolan BA are less effective in producing C-S-H, which plays an important role in increasing concrete strength [48]. In the corrosion acceleration process, akaganeite (β -FeOOH) and lepidocrocite (γ -FeOOH) are produced. The distinctive morphological characteristics of the four phases of rust are usually present among the corrosion products formed in the ocean-atmosphere: lepidocrocite, goethite, akaganeite, and magnetite [49]. The microcracks in Figure 16 in the BN specimen are more significant than the microcracks in the BA specimen, but the difference in crack size is not important. Microcracks in normal concrete and BA concrete have relatively small differences, and research shows that the addition of BA can reduce microcracks in concrete [50, 51, 52].

CONCLUSION

The research shows that adding BA to self-healing concrete reduces its compressive strength. A mixture with 30% BA lowers the strength by about 15% compared to regular concrete. Flexural strength is also affected by the corrosion process, but concrete mixed with BA and bacteria maintains better strength, especially at 20% BA after 48 hours of corrosion. However, as corrosion continues, flexural strength decreases with more BA content. NDT of impact echo and resistivity show that BA improves the concrete's ability to resist corrosion, with higher frequency and resistivity values than regular concrete. This means BA helps slow down the corrosion process. The best results were seen with 20% BA, which had the highest resistivity and frequency values.

ACKNOWLEDGMENT

This research was supported by the Ministry of Education, Culture, Research, and Technology (Indonesia), Directorate General of Higher Education, Research, and Technology for the project with number 107/E5/PG.02.00.PL/2024 and UMY.

REFERENCES

- [1] M. M. A. Elahi, M. M. Hossain, M. R. Karim, M. F. M. Zain, and C. Shearer, "A review on alkali-activated binders: Materials composition and fresh properties of concrete," *Construction and Building Materials*, vol. 260, p. 119788, 2020, doi. 10.1016/j.conbuildmat.2020.119788.
- [2] I. Bošković and A. Radivojević, "Life cycle greenhouse gas emissions of hemp-lime concrete wall constructions in Serbia: The impact of carbon sequestration, transport, waste production and end of life biogenic carbon emission," *Journal of Building Engineering*, Article vol. 66, 2023, Art no. 105908, doi. 10.1016/j.job.2023.105908.
- [3] K. C. Onyelowe and D. P. N. Kontoni, "The net-zero and sustainability potential of SCC development, production and flowability in concrete structures," *International Journal of Low-Carbon Technologies*, Article vol. 18, pp. 530-541, 2023, doi. 10.1093/ijlct/ctad033.
- [4] N. Akhtar *et al.*, "Ecological footprint and economic assessment of conventional and geopolymer concrete for sustainable construction," *Journal of Cleaner Production*, Article vol. 380, 2022, doi. 10.1016/j.jclepro.2022.134910.
- [5] H. G. Alcan, A. Benli, A. Öz, B. Bayrak, G. Kaplan, and A. C. Aydın, "Effective utilization of silica fume and waste colemanite in eco-sustainable prepacked geopolymers," *Construction and Building Materials*, vol. 457, pp. 139438, 2024, doi. 10.1016/j.conbuildmat.2024.139438.
- [6] M. Rafieizonooz, E. Khankhaje, and S. Rezaia, "Assessment of environmental and chemical properties of coal ashes including fly ash and bottom ash, and coal ash concrete," *Journal of Building Engineering*, vol. 49, pp. 104040, 2022, doi. 10.1016/j.job.2022.104040.
- [7] T. A. Abdalla, A. A. E. Hussein, Y. H. Ahmed, and O. Semmana, "Strength, durability, and microstructure properties of concrete containing bagasse ash – A review of 15 years of perspectives, progress and future insights," *Results in Engineering*, vol. 21, pp. 101764, 2024, doi. 10.1016/j.rineng.2024.101764.
- [8] H.-F. Li, Q.-Q. Yu, K. Zhang, X.-Y. Wang, Y. Liu, and G.-Z. Zhang, "Effect of types of curing environments on the self-healing capacity of mortars incorporating crystalline admixture," *Case Studies in Construction*

- Materials*, vol. 18, pp. e01713, 2023, doi. 10.1016/j.cscm.2022.e01713.
- [9] N. D. Tran, W. Saengsoy, and S. Tangtermsirikul, "Self-healing behavior of expansive mortars with fly ash and bottom ash," *Engineering Journal*, Article vol. 25, no. 2, pp. 121-133, 2021, doi. 10.4186/ej.2021.25.2.121.
- [10] A. S. Alemu, B. Y. Lee, S. Park, and H.-K. Kim, "Self-healing of Portland and slag cement binder systems incorporating circulating fluidized bed combustion bottom ash," *Construction and Building Materials*, vol. 314, pp. 125571, 2022, doi. 10.1016/j.conbuildmat.2021.125571.
- [11] S. Amirthaganesan, B. Ramesh, N. B. Veluru, and V. Kumar, *Influence of Bacteria Bacillus Subtilis and Its Effects on Compressive Strength of Concrete by Self-Healing Process*, 2020.
- [12] P. V. Yatish Reddy, B. Ramesh, and L. Prem Kumar, "Influence of bacteria in self healing of concrete - a review," in *Materials Today: Proceedings*, 2020, vol. 33, pp. 4212-4218, DOI. 10.1016/j.matpr.2020.07.233.
- [13] K. D. Wulandari *et al.*, "Effect of microbes addition on the properties and surface morphology of fly ash-based geopolymer paste," *Journal of Building Engineering*, Article vol. 33, 2021, doi. 10.1016/j.jobe.2020.101596.
- [14] K. W. Nindhita and A. Zaki, "State of the art: Correlation self-healing agent and corrosion on concrete," in *E3S Web of Conferences*, 2023, vol. 429, doi. 10.1051/e3sconf/202342905034.
- [15] M. Daniyal and S. Akhtar, "Corrosion assessment and control techniques for reinforced concrete structures: a review," *Journal of Building Pathology and Rehabilitation*, vol. 5, no. 1, pp. 1, 2019, doi. 10.1007/s41024-019-0067-3.
- [16] N. Renne, P. Kara De Maeijer, B. Craeye, M. Buyle, and A. Audenaert, "Sustainable Assessment of Concrete Repairs through Life Cycle Assessment (LCA) and Life Cycle Cost Analysis (LCCA)," *Infrastructures*, vol. 7, no. 10, pp. 128, 2022, doi. 10.3390/infrastructures7100128.
- [17] A. Zaki, M. A. Wibowo, S. A. P. Rosyidi, and K. Mahbubi, "Corrosion Analysis of Concrete using Resistivity Method," in *2023 International Workshop on Artificial Intelligence and Image Processing (IWAIIIP)*, 1-2 Dec. 2023 2023, pp. 428-432, doi. 10.1109/IWAIIIP58158.2023.10462756.
- [18] A. C. Rahita and A. Zaki, "Corrosion Analysis on Reinforcing Steel in Concrete Using the Eddy Current Method," in *Proceedings - 2023 3rd International Conference on Electronic and Electrical Engineering and Intelligent System: Responsible Technology for Sustainable Humanity, ICE3IS 2023*, 2023, pp. 476-480, doi. 10.1109/ICE3IS59323.2023.10335487.
- [19] A. Zaki, M. A. Fikri, C. A. Wibisono, and S. A. P. Rosyidi, "Evaluating Pre-Corrosion and Post-Corrosion of Oil Palm Shell Concrete with Non-Destructive Testing," in *Key Engineering Materials*, vol. 942, pp. 137-162, 2023, doi. 10.4028/p-9qfaiq.
- [20] A. Zaki, H. K. Chai, D. G. Aggelis, and N. Alver, "Non-destructive evaluation for corrosion monitoring in concrete: A review and capability of acoustic emission technique," *Sensors (Switzerland)*, Review vol. 15, no. 8, pp. 19069-19101, 2015, doi. 10.3390/s150819069.
- [21] H. Hamada, A. Alattar, B. Tayeh, F. Yahaya, and A. Adesina, "Sustainable application of coal bottom ash as fine aggregates in concrete: A comprehensive review," *Case Studies in Construction Materials*, vol. 16, pp. e01109, 2022, doi. 10.1016/j.cscm.2022.e01109.
- [22] P. Chindasiriphan, B. Meenyut, S. Orasutthikul, P. Jongvivatsakul, and W. Tangchirapat, "Influences of high-volume coal bottom ash as cement and fine aggregate replacements on strength and heat evolution of eco-friendly high-strength concrete," *Journal of Building Engineering*, vol. 65, pp. 105791, 2023, doi. 10.1016/j.jobe.2022.105791.
- [23] S. Ju, S. Bae, J. Jung, S. Park, and S. Pyo, "Use of coal bottom ash for the production of sodium silicate solution in metakaolin-based geopolymers concerning environmental load reduction," *Construction and Building Materials*, vol. 391, pp. 131846, 2023, doi. 10.1016/j.conbuildmat.2023.131846.
- [24] K. Tamanna, S. N. Raman, M. Jamil, and R. Hamid, "Coal bottom ash as supplementary material for sustainable construction: A comprehensive review," *Construction and Building Materials*, vol. 389, pp. 131679, 2023, doi. 10.1016/j.conbuildmat.2023.131679.
- [25] Y.-H. Kim, H.-Y. Kim, K.-H. Yang, and J.-S. Ha, "Effect of concrete unit weight on the mechanical properties of bottom ash aggregate concrete," *Construction and Building Materials*, vol. 273, pp. 121998,

- 2021, doi. 10.1016/j.conbuildmat.2020.121998.
- [26] M. Sadeghpour and M. Baradaran, "Effect of bacteria on the self-healing ability of fly ash concrete," *Construction and Building Materials*, vol. 364, p. 129956, 2023.
- [27] K. D. Wulandari *et al.*, "Effect of microbes addition on the properties and surface morphology of fly ash-based geopolymers paste," *Journal of Building Engineering*, vol. 33, pp. 101596, 2021, doi. 10.1016/j.jobe.2020.101596.
- [28] R. Mohan Rao Pannem, B. Bashaveni, and S. Kalaiselvan, "The effect of fly ash aggregates on the self-healing capacity of bacterial concrete," *Ain Shams Engineering Journal*, vol. 15, no. 1, pp. 102261, 2024, doi. 10.1016/j.asej.2023.102261.
- [29] A. Saxena, S. S. Sulaiman, M. Shariq, and M. A. Ansari, "Experimental and analytical investigation of concrete properties made with recycled coarse aggregate and bottom ash," *Innovative Infrastructure Solutions*, vol. 8, no. 7, pp. 197, 2023, doi. 10.1007/s41062-023-01165-y.
- [30] T.-P. Huynh and S.-H. Ngo, "Waste incineration bottom ash as a fine aggregate in mortar: An assessment of engineering properties, durability, and microstructure," *Journal of Building Engineering*, vol. 52, pp. 104446, 2022, doi. 10.1016/j.jobe.2022.104446.
- [31] N. Ankur and N. Singh, "Valorisation of bottom ash in concrete: serviceability, microstructural and sustainability characterisation," *Magazine of Concrete Research*, vol. 76, no. 21, pp. 1241-1265, 2024, doi. 10.1680/jmacr.23.00313.
- [32] T. Umar, M. Yousaf, M. Akbar, N. Abbas, Z. Hussain, and W. S. Ansari, "An Experimental Study on Non-Destructive Evaluation of the Mechanical Characteristics of a Sustainable Concrete Incorporating Industrial Waste," (in eng), *Materials (Basel)*, vol. 15, no. 20, 2022, doi. 10.3390/ma15207346.
- [33] P. Morla, R. Gupta, P. Azarsa, and A. Sharma, "Corrosion Evaluation of Geopolymer Concrete Made with Fly Ash and Bottom Ash," *Sustainability*, vol. 13, no. 1, pp. 398, 2021, doi. 10.3390/su13010398.
- [34] A. Zaki, H. Rahayu, D. A. Nugraha, S. A. P. Rosyidi, N. N. Kencanawati, and S. Fonna, "Resistivity Method Evaluation of Corroded OPS-Concrete," in *E3S Web of Conferences*, 2024, vol. 476: EDP Sciences, pp. 01037, doi. 10.1051/e3sconf/202447601037.
- [35] S. Hong *et al.*, "Determination of impressed current efficiency during accelerated corrosion of reinforcement," *Cement and Concrete Composites*, vol. 108, pp. 103536, 2020, doi. 10.1016/j.cemconcomp.2020.103536.
- [36] C. Liang *et al.*, "Effect of additional water content and adding methods on the performance of recycled aggregate concrete," *Construction and Building Materials*, vol. 423, pp. 135868, 2024, doi. 10.1016/j.conbuildmat.2024.135868.
- [37] M. J. Abdullah *et al.*, "The Strength and Thermal Properties of Concrete containing Water Absorptive Aggregate from Well-Graded Bottom Ash (BA) as Partial Sand Replacement," *Construction and Building Materials*, vol. 339, pp. 127658, 2022, doi. 10.1016/j.conbuildmat.2022.127658.
- [38] K. Mermerdaş, S. İpek, A. M. Anwer, Ş. Ekmen, and M. Özen, "Durability performance of fibrous high-performance cementitious composites under sulfuric acid attack," *Archives of Civil and Mechanical Engineering*, vol. 21, no. 4, pp. 147, 2021, doi. 10.1007/s43452-021-00298-0.
- [39] E. Chen, C. G. Berrocal, I. Fernandez, I. Löfgren, and K. Lundgren, "Assessment of the mechanical behaviour of reinforcement bars with localised pitting corrosion by Digital Image Correlation," *Engineering Structures*, vol. 219, pp. 110936, 2020, doi. 10.1016/j.engstruct.2020.110936.
- [40] L. Zhang, L. Sun, and L. Dong, "Experimental Study on the Relationship between the Natural Frequency and the Corrosion in Reinforced Concrete Beams," *Advances in Materials Science and Engineering*, vol. 2021, 2021, doi. 10.1155/2021/9976738.
- [41] C. Van Nguyen, P. Lambert, and V. N. Bui, "Effect of Locally Sourced Pozzolan on Corrosion Resistance of Steel in Reinforced Concrete Beams," *International Journal of Civil Engineering*, vol. 18, no. 6, pp. 619-630, 2020, doi. 10.1007/s40999-019-00492-5.
- [42] M. Madhan Kumar, D. Vijaya Ganapathy, V. Subathra Devi, and N. Iswarya, "Experimental Investigation on Fibre Reinforced Bacterial Concrete," *Materials Today: Proceedings*, vol. 22, pp. 2779-2790, 2020, doi. 10.1016/j.matpr.2020.03.409.
- [43] S. N. Priyom, M. M. Ismal, and W. Shumi, "Assessment on Strength Characteristics of Microbial Concrete by using Bacillus Subtilis as Self-healing Agent: A Critical Review," *International Journal of Sustainable*

- Construction Engineering and Technology*, vol. 11, no. 4, pp. 34-44, 2021, doi. 10.30880/ijscet.2021.11.04.004.
- [44] E. Stanaszek-Tomal, "Bacterial Concrete as a Sustainable Building Material?," *Sustainability*, vol. 12, no. 2, pp. 696, 2020, doi. 10.3390/su12020696.
- [45] P. Y. Wong, J. Mal, A. Sandak, L. Luo, J. Jian, and N. Pradhan, "Advances in microbial self-healing concrete: A critical review of mechanisms, developments, and future directions," *Science of The Total Environment*, vol. 947, pp. 174553, 2024, doi. 10.1016/j.scitotenv.2024.174553.
- [46] K. W. Nindhita, A. Zaki, and A. M. Zeyad, "Effect of Bacillus Subtilis Bacteria on the mechanical properties of corroded self-healing concrete," *Frattura ed Integrità Strutturale*, Article vol. 18, no. 68, pp. 140-158, 2024, doi. 10.3221/IGF-ESIS.68.09.
- [47] H. Ganesan, A. Sachdeva, P. Petrounias, P. Lampropoulou, P. K. Sharma, and A. Kumar, "Impact of Fine Slag Aggregates on the Final Durability of Coal Bottom Ash to Produce Sustainable Concrete," *Sustainability*, vol. 15, no. 7, pp. 6076, 2023, doi. 10.3390/su15076076.
- [48] B. Zhang, Y. Ma, Y. Liang, Y. Wang, and T. Ji, "Effect of Alkali Content on the High-Temperature Behavior of Alkali-Activated Slag Paste Containing MSWI Bottom Ash," *Journal of Materials in Civil Engineering*, vol. 36, no. 6, 2024, doi. 10.1061/JMCEE7.MTENG-16522.
- [49] Y. Fan *et al.*, "Evolution of rust layers on carbon steel and weathering steel in high humidity and heat marine atmospheric corrosion," *Journal of Materials Science & Technology*, vol. 39, pp. 190-199, 2020, doi. 10.1016/j.jmst.2019.07.054.
- [50] S. Poudel, S. Menda, J. Useldinger-Hoefs, L. E. Guteta, B. Dockter, and D. S. Gedafa, "The Use of Ground Coal Bottom Ash/Slag as a Cement Replacement for Sustainable Concrete Infrastructure," *Materials*, vol. 17, no. 10, pp. 2316, 2024, doi. 10.3390/ma17102316.
- [51] M. Vaičienė and E. Simanavičius, "The Effect of Municipal Solid Waste Incineration Ash on the Properties and Durability of Cement Concrete," (in eng), *Materials (Basel)*, vol. 15, no. 13, pp. 44862022, 2022, doi. 10.3390/ma15134486.
- [52] R. S. Edwin, S. Sulha, F. Masud, and W. Mustika, "Effect of mixing procedure and steam curing on the properties of Class C fly ash-cement based Geopolymer," *SINERGI*, vol. 28, no. 1, pp. 23-230, 2024, doi: 10.22441/sinergi.2024.1.003